Carbohydrate Polymers 87 (2012) 1176–1184

Contents lists available at SciVerse ScienceDirect

Carbohydrate Polymers

journal homepage: www.elsevier.com/locate/carbpol

Preparation and characterization of micelles of oligomeric chitosan linked to all-trans retinoic acid

Ali Fattahi[a,b,*], Mohammad-Ali Golozar[a], Jaleh Varshosaz[b,c,**], Hamid Mirmohammad Sadeghi[d], Mohammadhossein Fathi[a]

[a] Biomaterials Group, Department of Materials Engineering, Isfahan University of Technology, Isfahan 84146-83111, Iran
[b] Isfahan Pharmaceutical Sciences Research Centre, Isfahan University of Medical Sciences, Isfahan 81745-359, Iran
[c] Department of Pharmaceutics, School of Pharmacy, Isfahan University of Medical Sciences, Isfahan, Iran
[d] Biotechnology Department, School of Pharmacy and Pharmaceutical Sciences, Isfahan University of Medical Sciences, Isfahan, Iran

ARTICLE INFO

Article history:
Received 22 June 2011
Received in revised form 27 August 2011
Accepted 29 August 2011
Available online 10 September 2011

Keywords:
Oligochitosan
Derivatives
All trans retinoic acid (ATRA)
Polymer micelles
Cytotoxicity

ABSTRACT

New amphiphilic chitosan derivatives of all trans retinoic acid–chitosan (RA–chitosan) with different molar feeding ratios of all trans retinoic acid (ATRA) were synthesized. The degree of ATRA substitution ranged from 8.72% to 18.78%. The RA–chitosan formed micelles with an average size of 142.14–208.4 nm, and zeta potential of +27.25 to 34.48 mV. The critical association concentration (CAC) was found to range from 1.3×10^{-2} to 2.13×10^{-2} mg ml^{-1}. Upon evaluation, the RA–chitosan shows no significant cytotoxicity on Hela and HepG2 cells. Analysis of micelles loaded with ATRA revealed that the size of micelles decreased by increasing loaded drug content while zeta potential did not change. ATRA was released slowly over 3-day period, and drug content had no effect on the release rate. These phenomena make RA–chitosan micelles as a candidate for drug carrier.

1. Introduction

Polymeric micelles are colloidal carriers that promise enhancing the efficacy of hydrophobic drugs. The micelles have a core–shell structure with an internal core of hydrophobic segments surrounded by hydrophilic segment in an aqueous medium (Du, Wang, Yuan, Wei, & Hu, 2009; Nishiyama, Bae, Miyata, Fukushima, & Kataoka, 2005). Polymeric micelles are generally more stable than low-molecular-weight surfactant micelles, have a lower critical association concentration (CAC), and exhibit slower dissociation in aqueous environment (Du et al., 2009). Polymeric micelles can improve solubility of hydrophobic drugs including most anticancer agents. They also have a long circulation time, due to the steric hindrance caused by the presence of the hydrophilic shell. As a result, they can target the encapsulated drug to specific tissues, through either a passive or active mechanisms (Gaucher et al., 2005). They can also overcome drug resistance that develops in multidrug resistant (MDR) cells. It has been assumed that these micelles reduce the production of ATP, which is indispensable for p-glycoprotein activity. For these reasons, polymeric micelles are optimal candidates for cancer therapy (Liu, Li, Jiang, Zhang, & Ping, 2010).

Chitosan, a deacetylated form of chitin, consists of D-glucosamine and *N*-acetyl β-D-glucosamine linked by β(1→4) glycosidic bonds. Chitosan and its derivatives have attracted much attention because of their abundance in nature, biocompatibility, low toxicity, and synthesizability, as well as their hemostatic, bacteriostatic, fungistatic, and anticholesteremic properties. Although chitosan is insoluble in neutral aqueous medium, and cannot form micelles in water (Zhang, Ping, Zhang, & Shen, 2003), it has been reported that modified chitosans, e.g., chitosan taurocholate (Muzzarelli et al., 2006), *N*-alkyl-*O*-sulfate chitosan (Zhang et al., 2003), *N*-octyl-*N*-(2-carboxyl cyclohexamethenyl) chitosan (Liu et al., 2010), linoleic–chitosan (Liu, Chen, & Park, 2005), cholesterol–chitosan (Yuan, Li, & Yuan, 2006), oleoy-carboxymethyl chitosan (Li, Zhang, Meng, Chen, & Ren, 2010), *N*-acetyl, and stearic-chitosan (Ye, Hu, & Yuan, 2004) can produce micelles. The low solubility and high viscosity of chitosan hamper its capacity for systemic nanoparticle drug delivery. To overcome these two disadvantages, many researchers have focused on low-molecular-weight chitosan oligosaccharide (Du et al., 2009; Hu, Ren, Yuan, Du, & Zeng, 2006; Hu, Zhao, et al., 2006; Hu, Liu,

* Corresponding author at: Biomaterials Group, Department of Materials Engineering, Isfahan University of Technology, Isfahan 84146-83111, Iran. Tel.: +98 311 391 2750; fax: +98 311 391 2752.
** Corresponding author at: Isfahan Pharmaceutical Sciences Research Centre, Isfahan University of Medical Sciences, Isfahan 81745-359, Iran. Tel.: +98 311 792 2579; fax: +98 311 668 0011.
E-mail address: a.fatahi.a@gmail.com (A. Fattahi).

0144-8617/$ – see front matter © 2011 Elsevier Ltd. All rights reserved.
doi:10.1016/j.carbpol.2011.08.093

Du, & Yuan, 2009). The fact that chitosan oligosaccharide inhibits tumour-induced angiogenesis makes it a promising anticancer drug carrier (Harish Prashanth & Tharanathan, 2005).

Recently, polymeric micelles have attracted considerable attention to the potential advantages of hydrophobic drugs (especially anticancer drugs) that are covalently linked to a polymer. The conjugation of hydrophobic drugs with water-soluble polymers improves their aqueous solubility and decreases their renal clearance. Some studies have shown that covalently linked hydrophobic drugs not only form the hydrophobic core of micelle but also function in the targeted cells (Chen, McRae, Parelkar, & Emrick, 2009; Fan et al., 2010; Hu et al., 2009; Lee, Lee, & Park, 2008; Veronese et al., 2005).

We hypothesize that using an anticancer drug as hydrophobic part of the micelle can allow the co-deliver of two or even more anticancer drugs to tumours and cancer cells. Co-delivery of anticancer drugs not only can decrease side effects but also overcomes drug resistance (Agarwal & Kaye, 2003).

All-trans retinoic acid (ATRA), the most biological active form of retinol (vitamin A), plays an essential role in the induction of cell differentiation and the arrest of cell proliferation. It has been used in stem cell engineering and cancer therapy. Currently, ATRA is effectively used in differentiation therapy for acute myelogeneous lukemia (Lübbert, Müller Tidow, Hofmann, & Koeffler, 2008; Schug, Berry, Shaw, Travis, & Noy, 2007; Tang & Gudas, 2011).

Despite all its advantages, the use of ATRA has been limited because of its disadvantages, which include poor water solubility, physicochemical instability, drug resistance, hypertriglyceridermia, mucocutaneous dryness and headache (Kim, Choi, Jeong, Jang, & Nah, 2006). Furthermore, the concentration of ATRA in circulating blood has been shown to gradually decrease after its oral administration or intravenous injection. This decrease is attributed to ATRA being metabolised in the liver by an RA-inducible P-450 cytochrome called p450AI (Coradini, 2007; Seo et al., 2004).

To overcome these disadvantages, ATRA has been encapsulated in micro/nanoparticles such as chitosan micro/nanoparticles, liposomes and polymeric micelles (Díaz, Vargas, & Gätjens-Boniche, 2006; Kim et al., 2006; Li, Qi, Maitani, & Nagai, 2009; Seo et al., 2004).

In this present study, ATRA was grafted to water-soluble chitosan oligosaccharide for the purpose of synthesizing ATRA–chitosan conjugation with different graft ratios of ATRA, creating a novel micellar form of chitosan that is compatible with drug delivery.

2. Materials and methods

2.1. Materials

The chitosan oligosaccharide (90% deacetylated; verified by ^{1}HNM0052, Mw = 8.6 kDa; verified by CTO-20 AC-Shimadzu high performance liquid chromatography using refractive index detector and Ultrahydrogel 250 column, and PEG as standard) was supplied by Yuhuan Marine Biochemistry Co., Ltd., Zhejiang, China. Dicyclohexylcarbodiimide (DCC), N-hydroxysuccinimide (NHS), ATRA, pyrene and anhydride dimethyl sulfoxide (DMSO), as well as other compounds were purchased from Sigma Chemical Co. (USA).

2.2. Synthesis of RA–chitosan and preparation of RA–chitosan micelles

The chemical conjugate of RA–chitosan was synthesized by the coupling reaction of the carboxyl group of ATRA with the amine group of chitosan in the presence of DCC and NHS (Fig. 1). Specifically, chitosan (0.3 mmol) was dissolved in 5 ml water, after which 40 ml DMSO was added to chitosan solution. ATRA with the molar feeding ratios of 10%, 25%, and 50% (which mean the molar ratio of ATRA to D-glucosamine units of chitosan), DCC (1.5× ATRA in mol) and NHS (1.5× ATRA in mol) were dissolved in 5 ml of dry DMSO. The solutions were stirred thoroughly for 6 h prior to condensation reaction.

The two reactant solutions were mixed, and stirred at room temperature for 24 h, while protected from light. After the resulting solution was filtered to remove insoluble by-products (e.g., dicyclohexylurea), it was precipitated in acetone and then washed three times with acetone. To further increase purification, precipitated product was dissolved in deionized (DI) water and dialyzed using a dialysis membrane (Sigma, cote off 2 kDa) against ethanol for 2 days and then water for 1 day. The synthesized RA–chitosan with 10%, 25% and 50% molar feeding ratio of ATRA were encoded as RA–chitosan-10, RA–chitosan-25, and RA–chitosan-50, respectively, for further evaluation.

To prepare the micelles, RA–chitosan was suspended in water or PBS buffer (pH 7.4) at 1 mg ml^{-1}, followed by sonication using probe type sonicator (Sonopuls HD 3200, Bandeline, Germany) at 60 W for 2 min (2 s pulse on and 2 s pulse off) (Lee, Kwon, Kim, Jo, & Jeong, 1998). Sonication was repeated three times to obtain optically clear solution. To avoid the heat build-up, the sonication was done in an ice bath.

2.3. Physicochemical characterization of RA–chitosan and micelles

A ^{1}H NMR analysis was performed using Bruker Biospin (AC-400, Germany). 5 mg ml^{-1} of oligochitosan and RA–chitosan dissolved in D_2O, and ATRA dissolved in deutriated DMSO, were measured using an NMR spectrometer.

FTIR spectra were recorded on Fourier-transform infrared spectrometer (WQS-510/520, Raileigh, China) using KBr discs.

The degree of substitution (DS) for the RA–chitosan was assayed using the 2,4,6-trinitrobenzene sulfonic acid (TNBS) test. Specifically, 200 μl of 4 mg ml^{-1} modified or unmodified chitosan was incubated with 200 μl of 4% $NaHCO_3$ and 200 μl of 0.1% TNBS at room temperature for 8 h. UV absorbance was determined at 343 nm, using 0.033% TNBS in 1.3% $NaHCO_3$ as a blank (Loretz & Bernkop-Schnürch, 2006).

2.3.1. Critical association concentration (CAC) of RA–chitosan micelles

The CAC of the RA–chitosan micelles was determined by fluorescence measurement using pyrene as the probe (Wolszczak & Miller, 2002). The pyrene solutions (6.0×10^{-6} M) were prepared in acetone and stored at −20 °C until used. 300 μl of pyrene solution was added to 3 ml of aqueous solutions containing different concentrations of RA–chitosan micelles (2.0×10^{-3} to 0.5 mg ml^{-1}) and incubated at 37 °C overnight. The resulting solutions were gently shaken to evaporate the acetone.

The fluorescence spectra of the solution were recorded on a spectrofluorometer (LS-3B, Perkin-Elmer, USA) at room temperature. The excitation wavelength was 336 nm and the emissions were monitored at wavelengths ranging from 360 to 450 nm. Depending on the pyrene emission spectra, the intensity ratio of the first peak (I_1, 377 nm) to the third peak (I_3, 390 nm) was used to calculate the CAC.

2.3.2. Particle size and zeta potential measurements

The particle size and zeta potential of the RA–chitosan micelles were measured by a zetasizer (Zetasizer-ZEN3600 Malvern Instrument Ltd., Worchestershire, UK). All particle-size measurements were performed in PBS buffer (pH 7.4) using a He–Ne laser beam

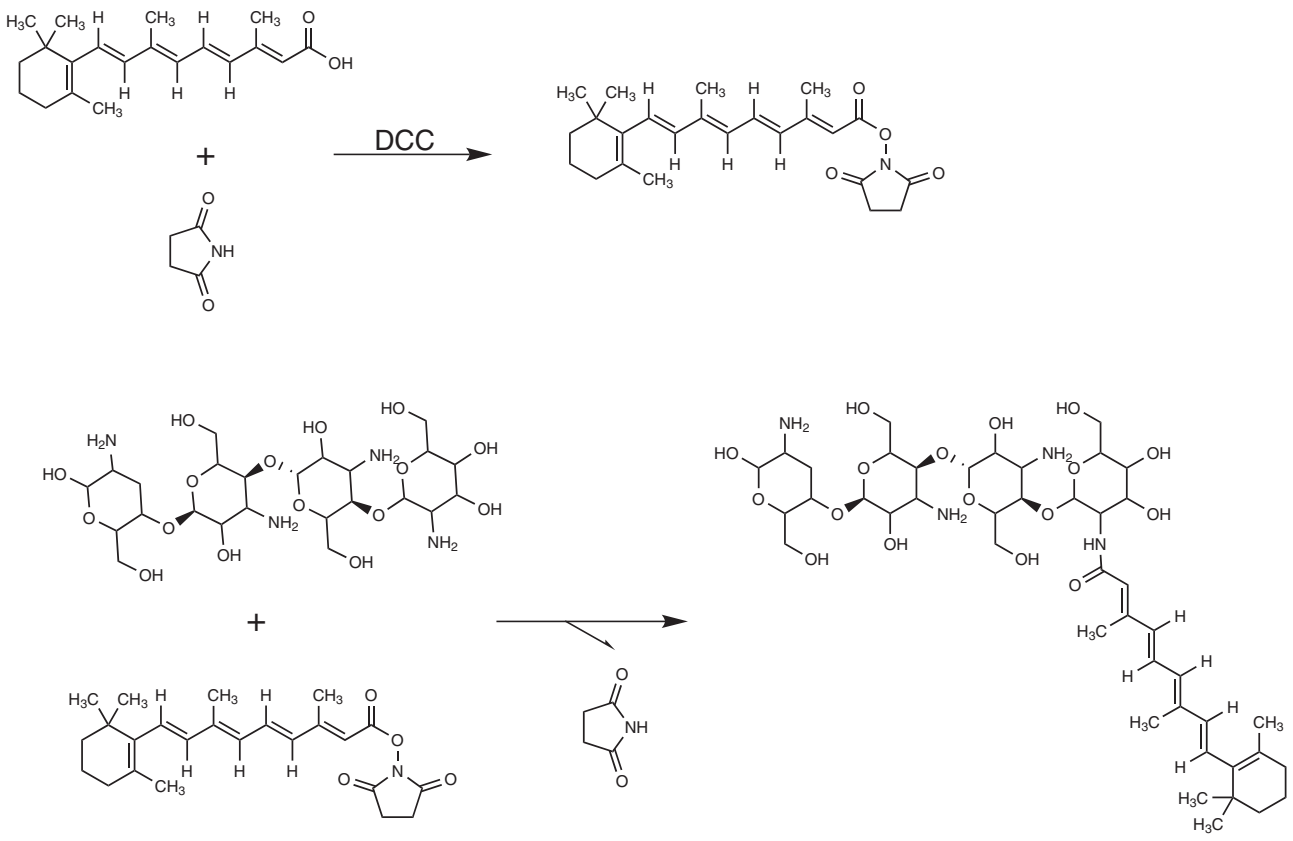

Fig. 1. Synthesis of ATRA-grafted chitosan oligosaccharide (RA–chitosan).

at 658 nm with a scattering angle of 130°. To study the colloidal stability of the RA–chitosan micelles, their size was monitored for 2 weeks. The device calculated the zeta potential of the nanomicelles from their electrophoretic mobility using Smoluchowski's equation (Dong et al., 2009). All the experiments were performed in triplicate.

2.3.3. Cell culture

HepG2 and Hela cells were obtained from the Pasteur Institute in Iran. They were maintained in RPMI-1640 supplemented by 10% (v/v) FBS (fetal bovine serum) and penicillin/streptomycin (50 IU ml^{-1}, 500 μg ml^{-1}) at 37 °C in a humidified atmosphere of 5% CO_2. The cells were subcultured regularly using trypsin/EDTA.

2.3.4. In vitro cytotoxicity

A cytotoxicity test was used to evaluate the *in vitro* viability of the RA–chitosan against HepG2 and Hela cells. Specifically, the HepG2 and Hela cells were plated in 96-well plates and grown for 24 h. The cells were exposed to several chitosan concentrations, free ATRA and RA–chitosan at 37 °C for another 24 or 96 h. At the end of the incubation period, 20 ml of MTT solution with a concentration of 5 mg ml^{-1} was added and incubated for a further 3 h at 37 °C. Each well was then washed with 50 ml of PBS after the medium containing the unreacted MTT was removed. Then, 150 ml of DMSO was added to each well to dissolve the formazan crystals. Finally, the absorbance of the dissolved formazan was measured at 540 nm using an ELISA reader (Bio-Rad, Model 680, USA) (Yokoyama, Okano, Sakurai, Suwa, & Kataoka, 1996; Yoo & Park, 2001). All the experiments were performed in triplicate.

2.4. Preparation and characterization of ATRA loaded RA–chitosan micelles

ATRA served as a hydrophobic model drug to evaluate the RA–chitosan micelles as carrier of anticancer drugs. The drug-loaded RA–chitosan micelles were prepared by dialysis method. Specifically, 800 and 200 μl of a 1 mg ml^{-1} ATRA solution in DMSO were added to 4 ml of a 1 mg ml^{-1} of RA–chitosan-50 aqueous solution to achieve weight feeding ratios of 20% and 5%, respectively. The mixtures were then sonicated for 2 min by a probe sonicator (2 s pulse on and 2 s pulse off) in an ice bath. The mixture was then dialyzed against water for 24 h. Next, the unloaded drug was separated by centrifuging at 4000 rpm for 10 min (Du et al., 2009).

To estimate the content of the loaded drug, 100 μl of the drug-encapsulated micelle solution was added to 900 μl DMSO and vortexed for 1 min to break down the micelles (Kim et al., 2006). The ATRA content was measured by a UV–Vis spectrophotometer (UV mini-1240 CE, Shimadzu, Japan) using the standard curve of ATRA concentration versus absorbance at 360 nm, in a mixture of 10% DMSO to 90% water. Unloaded micelles were used as controls. Drug content (DC) and loading efficacy (LE) were calculated by the following equations (Li et al., 2009):

$$\mathrm{DC} = \left[\frac{W}{(W_{\mathrm{bm}} + W)}\right] \times 100 \quad (1)$$

$$\mathrm{LE} = \frac{W}{W_{\mathrm{o}}} \times 100 \quad (2)$$

where W is the weight of the loaded drug, W_{bm} is the weight of the control micelles, and W_{o} is the weight of the initial feeding drug.

The FTIR, sizes and zeta potentials of the drug-loaded micelles were assessed as described in Sections 2.3 and 2.3.2 above.

Table 1
(A) Characteristics of RA–chitosan micelles and (B) characteristics of ATRA loaded RA–chitosan-50 micelles.

(A)

Code name	DS%	Size (nm)	Zeta (mV)	CAC (mg ml^{-1})
CHRA–50	18.78 ± 0.86	142.14 ± 5.06	27.25 ± 6.31	1.3×10^{-2}
CHRA–25	12.77 ± 0.44	166.6 ± 2.45	31 ± 1.31	1.8×10^{-2}
CHRA–10	8.72 ± 0.59	208.4 ± 24.64*	34.48 ± 3.92	2.13×10^{-2}

(B)

Feeding ratio ($W_{ATRA}/W_{RA-chitosan-50}$)	Loading efficacy	Loading content	Size	Zeta potential
5%	60.27 ± 8.57%	3.02 ± 0.43%	193.1 ± 4.2*	33.73 ± 2.25
20%	56.58 ± 9.7%	9.33 ± 2.4%*	154.1 ± 0.9	32.57 ± 1.4

* The main difference is significant at the 0.05 level.

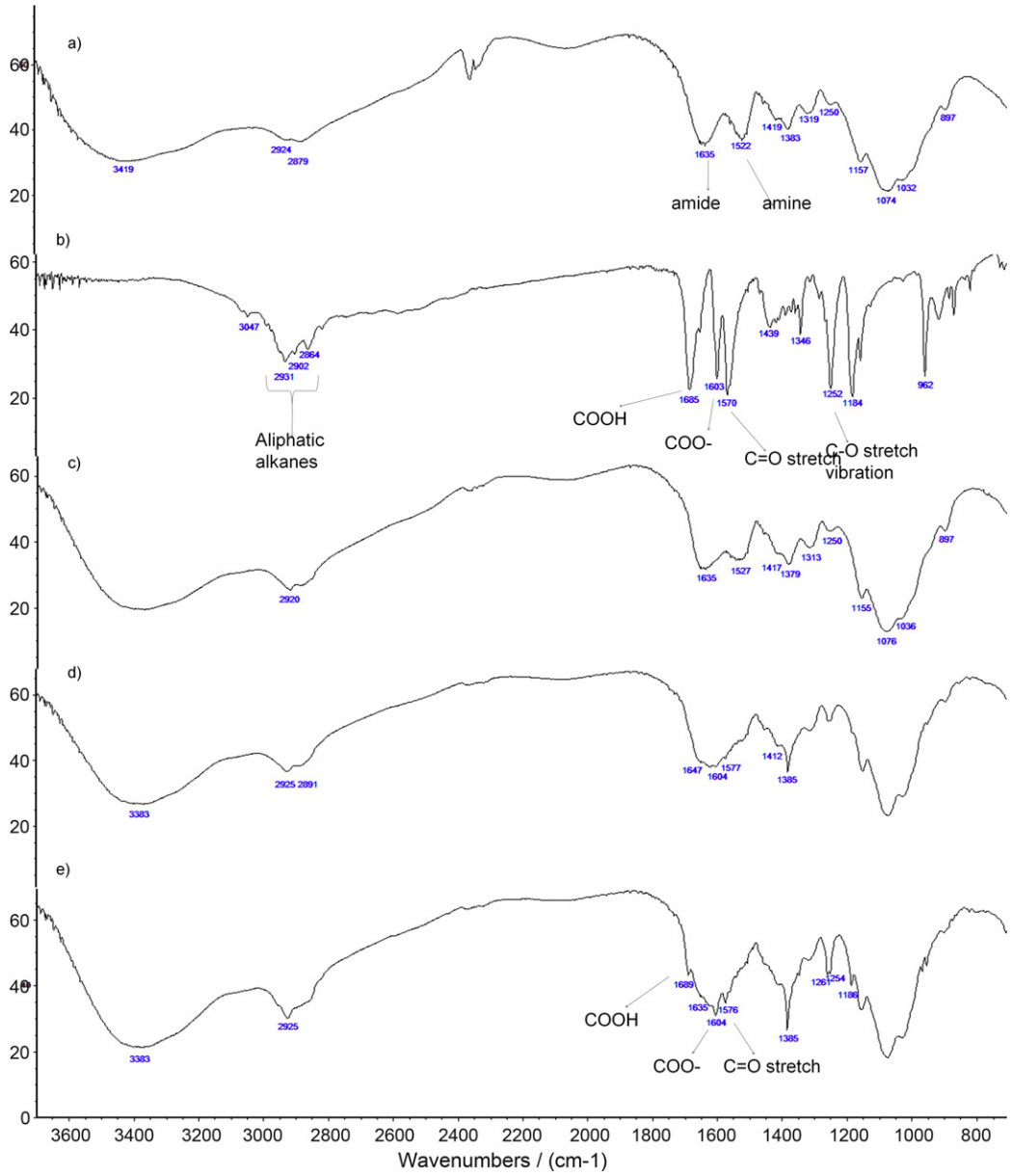

Fig. 2. FTIR of chitosan and its derivatives: (a) chitosan, (b) ATRA, (c) RA–chitosan-50, (d) ATRA loaded RA–chitosan-50 micelles with 5% molar feeding amount and (e) ATRA loaded RA–chitosan-50 micelles with 20% molar feeding amount.

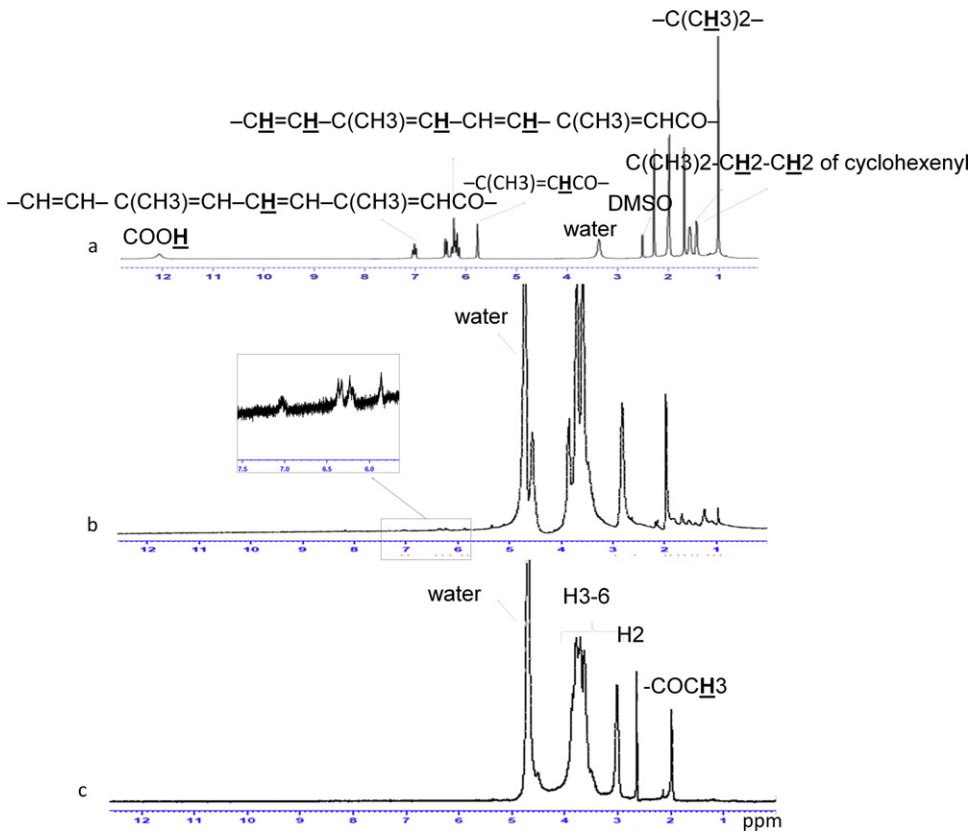

Fig. 3. ^{1}H NMR spectra: (a) ATRA, (b) RA–chitosan, and (c) chitosan.

2.4.1. In vitro drug release study

The *in vitro* release of ATRA was achieved using PBS (pH = 7.4) as the release medium. 2 ml of loaded micelles were placed in a dialysis membrane bag (cut-off 2000 Da). The whole bag was sunk in 20 ml of release medium at 37 °C while being stirred. To assure that the sinking was adequate, the whole release medium was withdrawn at predetermined time intervals and replaced by a fresh medium.

The ATRA concentration in PBS was determined by UV spectrophotometry, using standard curve of ATRA in PBS at wavelength of 360 nm.

3. Results and discussion

3.1. Synthesis of RA–chitosan

RA–chitosan was successfully synthesized by the coupling reaction between the amino groups of chitosan oligosaccharide and the carboxyl group of ATRA. The degree of substitution (DS%) of the RA–chitosan is shown in Table 1A. Conjugation of RA–chitosan was confirmed using FTIR and ^{1}H NMR spectra. A comparison of the chitosan and ATRA FTIR spectra revealed in the RA–chitosan spectrum an increase in the intensity of the amide group peak at 1635 cm^{-1} and a decrease in the intensity of the amine group at 1522 cm^{-1}. The peak of the protonated carboxyl groups of ATRA completely disappeared in the RA–chitosan spectrum, whereas the intensity of the aliphatic alkanes at 2931 peak increased (Fig. 2).

The ^{1}H NMR spectrum was also used to confirm the binding between ATRA and chitosan oligosaccharide, as is illustrated in Fig. 3. It is clear that the proton peak of the COOH of ATRA (chemical shift 12.064 ppm) was observed in its ^{1}H NMR spectrum, but it disappeared in the ^{1}H NMR spectrum of RA–chitosan. This result indicates the presence of a covalence bond between ATRA and chitosan. Furthermore, the RA–chitosan spectrum revealed the emergence of new peaks at δ = 0.936 (–C(C**H**3)2– of cyclohexenyl), 5.849 (–C(CH3)=C**H**CO–), 6.25–6.3384 (–C**H**=C**H**–C(CH3)=C**H**–CH=C**H**–C(CH3)=CHCO–) and 7.056 (–CH=CH–C(CH3)=CH–C**H**=CH–C(CH3)=CHCO–), all attributable to ATRA.

3.2. Physicochemical properties of RA–chitosan micelles

In the aqueous solvents, the hydrophobic ATRA moieties of the RA–chitosan were assembled themselves in hydrophobic cores, while these cores were surrounded by hydrophilic chitosan backbones, to achieve the lowest Gibbs free energy level. The spontaneous self-aggregation of the RA–chitosan in the aqueous medium was determined by the dye solubilization method using pyrene as the probe molecule. The emission spectra of pyrene depend strongly on the polarity of the microenvironment; in polar solvents, the intensity of the first energy band (377 nm, I_1) of the pyrene emission spectrum is higher than that of the third (390 nm, I_3) whereas in a hydrophobic environment, I_3 is higher than I_1. Therefore, when micelles are formed in an aqueous medium, the pyrene tends to locate itself inside the hydrophobic core, increasing I_3 intensity. As a result, the ratio of I_1 to I_3 can be used to determine the CAC.

Micelle solutions are diluted in the body fluids; as a consequence, they are expected to be disassociated. Thus, the lower the CAC value, the more stable the micelles in the body fluids (Bian, Jia, Yu, & Liu, 2009). Fig. 4a shows the variation in the fluorescence intensity ratio (I_1/I_3) against the logarithm of RA–chitosan micelles

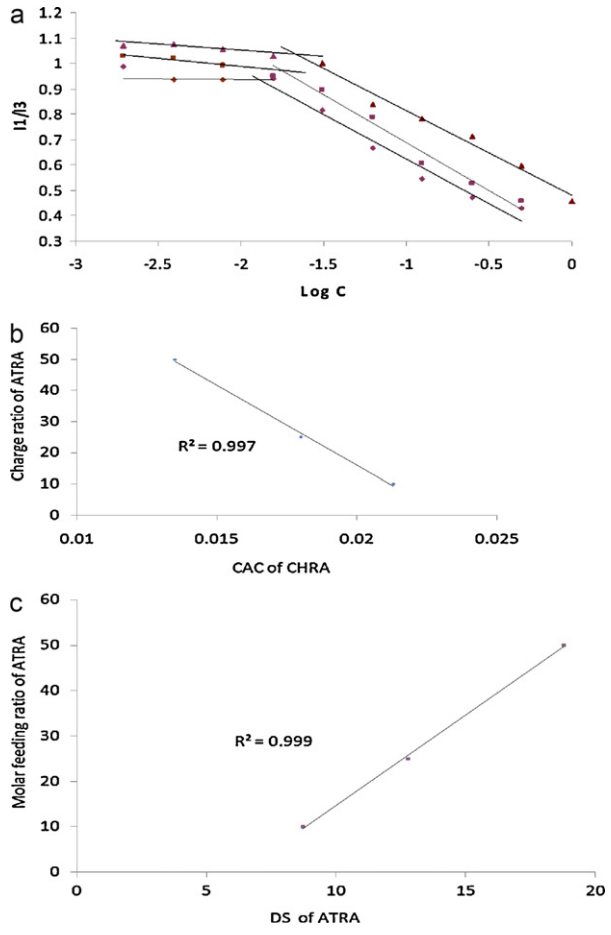

Fig. 4. (a) Intensity ratio plots of I_1/I_3 of pyrene versus log C for RA–chitosan micelles: RA–chitosan-10 (▲), RA–chitosan-25 (■), and RA–chitosan-50 (♦). The plots of ATRA molar feeding ratio versus (b) CAC and (c) DS.

concentration. At concentrations lower than the CAC, the ratios were approximately the same, whereas in concentrations higher than the CAC, a linear decrease in the ratios was observed with increasing RA–chitosan micelles concentration. The CAC values were defined as the crossover point of the two straight lines of each RA–chitosan micelle (Na, Park, Kim, & Bae, 2000). The CAC value of RA–chitosan micelles decreased as the graft ratio of the polymer increased (Table 1A). Thus, there was a direct correlation between the ATRA feeding ratio and CAC, at least for the values used in this study. The absolute values of correlation coefficient (R) were larger than 0.9 suggesting a linear relationship (Fig. 4b).

The hydrophobic interaction between the ATRA moieties of the RA–chitosan micelles increased as the graft ratio of the RA–chitosan increased, a trend which favours micelles formation at lower RA–chitosan concentrations. Despite, Fig. 4c shows relationship of DS% and feeding ratio; the slope of the line is less than one which means the graft yield decreases as the feeding ratio increases.

In this study, the RA–chitosan-50 had the lowest CAC, allowing micelles to be formed with a 13.5 μg ml^{-1} concentration, around 170 times lower than the concentrations needed to form micelles with low-molecular-weight surfactants micelles, e.g., sodium dodecyl sulfate (SDS) which has a CAC of 2.3 mg ml^{-1} (Bian et al., 2009). This result clearly indicates that the RA–chitosan-50 polymer can form micelles even in highly diluted solutions.

The RA–chitosan micelles were prepared by dissolving a RA–chitosan in distilled water using a probe-type sonicator. Table 1A summarizes the properties of micelles at 1 mg ml^{-1} of

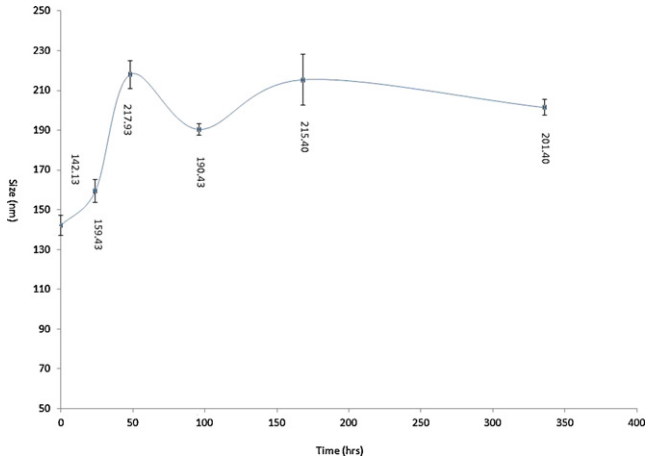

Fig. 5. Particle size of RA–chitosan-50 micelles (1 mg ml^{-1}) during the time as function of colloidal stability.

RA–chitosan concentration. It was found that the size and zeta potential of the RA–chitosan micelles declined as the graft ratio of the RA–chitosan increased ($p < 0.05$). The RA–chitosan-50 micelles had the smallest average size and zeta potential: 142.14 ± 5.06 nm and +27.25 ± 6.31 mV, respectively. The reduction of micelle size resulted from the enhanced hydrophobic interaction, which was caused by an increase in the graft ratio. In fact, with this increase and the resulting polymer hydrophobicity, the micelles formed in a more tightly packed core. Monitoring the size of the RA–chitosan micelles during the time indicates that their colloidal stability depended on the CAC. The average size of the RA–chitosan-50 micelles increased only from 142.13 to 217.93 nm in the first 24 h, and there was no increase at all during the next 2 weeks (Fig. 5). On the other hand, the RA–chitosan-10 and RA–chitosan-25 micelles showed a sharp increase in size from approximately 160–200 nm to 1 μm, during the same 24 h period at room temperature (data not shown). The difference is probably attributable to the strong ionic environment of PBS which causes the RA–chitosan-10 and RA–chitosan-25 micelles to disassociate and re-aggregate, similar to what López-León, Carvalho, Seijo, Ortega-Vinuesa, and Bastos-González (2005) have found in a comparable situation. On the other hand, the tightly packed RA–chitosan-50 micelles showed definite stability in the buffer solution.

3.3. *In vitro cytotoxicity*

The viability data for the Hela and HepG2 cells at 24 h and 96 h are shown in Fig. 6a and b. We have investigated the viability of these cells in the presence of the RA–chitosan and free ATRA with a concentration level similar to that of the micelles. ATRA is known to inhibit mitosis and the proliferation of Hela and HepG2 (Díaz et al., 2006; Mao, Liu, Chen, Li, & Zhou, 2006). Thus, to evaluate these effects, viability was investigated at both 24 and 96 h (Díaz et al., 2006; Kucukzeybek et al., 2008). Neither the RA–chitosan nor free ATRA were shown to cause any significant cytotoxicity on the cells, even in concentrations as high as 100 μg ml^{-1}. Interestingly, at 96 h, chitosan oligosaccharide was found to create more toxicity than RA–chitosan on Hela, although the difference was not statistically significant. This result could be attributable to the lower positive charge of RA–chitosan (Fig. 6A.1 and A.2). Studies of cationic carriers in gene delivery show that the positive charge of these carriers causes cytotoxicity (Lv, Zhang, Wang, Cui, & Yan, 2006). In the case of free ATRA, a concentration as small as 26.9 μg ml^{-1}, even not to a meaningful extent, could decrease viability. Although the

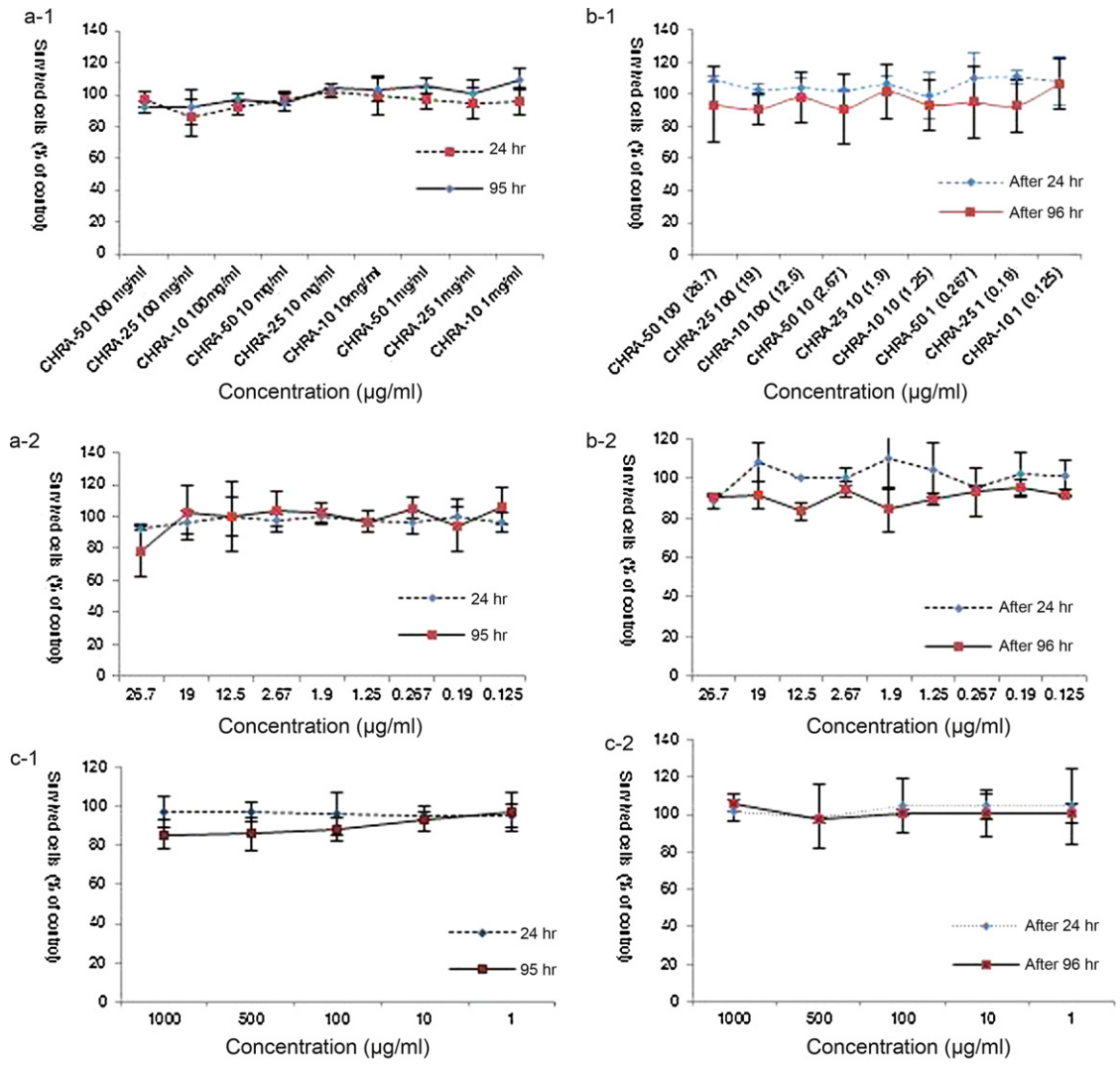

Fig. 6. MTT assay for cytotoxicity of RA–chitosan on Hela cell (A-1) and HepG2 cell (B-1), ATRA on Hela cell (A-2) and HepG2 cell (B-2) and chitosan oligosaccharide on Hela cell (C-1) and Hepg2 cell (C-2).

concentration of ATRA we used was smaller than its half maximal inhibitory concentration (IC_{50}), it is still capable of increasing the cytotoxicity of other anticancer drugs such as Taxol and arsenic trioxide (AsO_3) (Kucukzeybek et al., 2008; Lin, Li, Xiao, Lin, & Yang, 2005). Thus, in cancer therapy, RA–chitosan micelles may be considered a promising targeting delivery system for drugs.

3.4. Preparation and characterization of drug-loaded RA–chitosan micelles

The drug-encapsulated micelles were prepared by dialysis method and then lyophilized to turn them into powder. The chemico-physical characteristics of these drug-loaded micelles is summarized in Table 1B. Increasing the drug feeding amount had no significant effect on loading efficiency, although drug content was significantly enhanced. This increase in drug content caused an increase in molecular hydrophobicity, which resulted in more tightly packed micelles, shrinkage of the particles, and decrease in their water content. Collectively, these effects resulted in a decrease in the size of the loaded micelles, along with an increase in the feeding amount. These findings are consistent with those of other studies (Na et al., 2000). Increasing the drug content did not significantly change the zeta potential, which indicates that there were no ionic interactions between RA–chitosan micelles and ATRA. Thus, most of the drug was loaded in the micelle's core rather than the shell. According to loaded micelles FTIR, peaks at 1252, 1570, and 1685 cm^{-1} are attributable to C–O stretch vibration, C=O stretch, and the COOH of free ATRA, respectively. The intensity of the peaks was enhanced by increasing the feeding amount (Fig. 2d and e). This result lends further supports to the above hypothesis, emphasizing that most of the drug is encapsulated in the core and that there are no ionic interactions among the micelles shells.

3.4.1. In vitro drug release from RA–chitosan-50 micelles

Fig. 7 shows that it took 3 days for more than 70% of the drug to be released, and there was no significant change in the release profile when drug content was increased. This slow and prolonged release is attributable to the hydrophobic nature of ATRA, and perhaps as well to crystallization inside the micelle's core (Kim et al., 2006; Na et al., 2000). Considering that the micelles retained the drug inside the core due to the slow drug leakage, it can be concluded that the drug is released only when the micelles are taken up and the chitosan molecules are enzymatically degraded within the tumoural cells. This process increases the concentration of the drug in tumours by enhanced permeability and retention (ERP) effect.

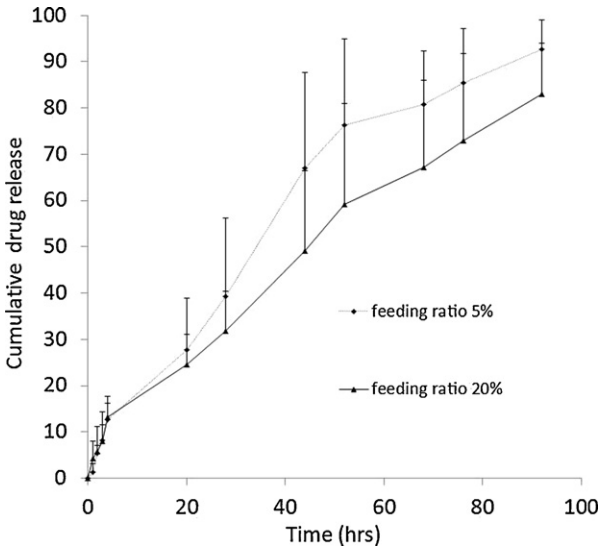

Fig. 7. ATRA cumulative release curve from RA–chitosan-50 micelles for 96 h at 37 °C.

4. Conclusion

The chemical conjugates of RA–chitosan as a novel derivative of chitosan oligosaccharide were synthesized using a coupling reaction of water-soluble chitosan oligosaccharide and ATRA with different graft ratios. The self-aggregation process created nano-sized polymeric micelles in an aqueous medium, and the resulting micelles were stable for a long time in PBS. The size of the micelles was controlled by DS. Colloidal stability of the RA–chitosan micelles was increased by decreasing the CAC. The cytotoxicity of the RA–chitosan against HepG2 and Hela cells suggests that the modified chitosan oligosaccharide was non-toxic. Loading efficiency and drug content were 60.27% and 3.02%, respectively, for the 5% feeding ratio, and 56.58% and 9.33%, respectively, for the 20% feeding ratio. The appearance of characteristic peaks of free ATRA in the FTIR of the loaded micelles, along with the zeta potential, indicates that the drug molecules were predominantly encapsulated in the micelle's core rather than the outer shell, because there was no significant ionic interaction with the outer shell. The size of the loaded micelles was decreased by increasing the feeding amount of the loaded drug while the zeta potential did not change significantly. This result suggests that increasing DS resulted in greater hydrophobicity and hence tightly packed hydrophobic core. This process shrunk the micelles, i.e., reduced their size. The release of ATRA lasted up to 3 days and there was no significant difference in the release rate when the drug content was increased. Because of their low CAC value, colloidal stability, lack of cytotoxicity, good loading efficiency, and sustained release of the drug, RA–chitosan-50 micelles are an excellent candidate for a carrier that delivers drug to cancerous tissues.

Acknowledgment

This work is supported by the research grant No. 289171 from Isfahan Pharmaceutical Sciences Research Centre of the Isfahan University of Medical Sciences, and Isfahan University of Technology.

References

Agarwal, R. & Kaye, S. B. (2003). Ovarian cancer: Strategies for overcoming resistance to chemotherapy. *Nature Reviews Cancer*, *3*, 502–516.

Bian, F., Jia, L., Yu, W. & Liu, M. (2009). Self-assembled micelles of N-phthaloylchitosan-G-polyvinylpyrrolidone for drug delivery. *Carbohydrate Polymers*, *76*(3), 454–459.

Chen, X. J., McRae, S., Parelkar, S. & Emrick, T. (2009). Polymeric phosphorylcholine–camptothecin conjugates prepared by controlled free radical polymerization and click chemistry. *Bioconjugate Chemistry*, *20*(12), 2331–2341.

Coradini, D. (2007). New chemical strategies for overcoming ATRA resistance in Apl cells. *Leukemia Research*, *31*(3), 291–292.

Díaz, C., Vargas, E. & Gätjens-Boniche, O. (2006). Cytotoxic effect induced by retinoic acid loaded into galactosyl-sphingosine containing liposomes on human hepatoma cell lines. *International Journal of Pharmaceutics*, *325*(1–2), 108–115.

Dong, L., Xia, S., Luo, Y., Diao, H., Zhang, J., Chen, J., et al. (2009). Targeting delivery oligonucleotide into macrophages by cationic polysaccharide from *Bletilla striata* successfully inhibited the expression of Tnf-[alpha]. *Journal of Controlled Release*, *134*(3), 214–220.

Du, Y. Z., Wang, L., Yuan, H., Wei, X. H. & Hu, F. Q. (2009). Preparation and characteristics of linoleic acid-grafted chitosan oligosaccharide micelles as a carrier for doxorubicin. *Colloids and Surfaces B: Biointerfaces*, *69*(2), 257–263.

Fan, N., Duan, K., Wang, C., Liu, S., Luo, S., Yu, J., et al. (2010). Fabrication of nanomicelle with enhanced solubility and stability of camptothecin based on [alpha],[beta]-poly[(N-carboxybutyl)-L-aspartamide]-camptothecin conjugate. *Colloids and Surfaces B: Biointerfaces*, *75*(2), 543–549.

Gaucher, G., Dufresne, M. H., Sant, V. P., Kang, N., Maysinger, D. & Leroux, J. C. (2005). Block copolymer micelles: Preparation, characterization and application in drug delivery. *Journal of Controlled Release*, *109*(1–3), 169–188.

Harish Prashanth, K. V. & Tharanathan, R. N. (2005). Depolymerized products of chitosan as potent inhibitors of tumor-induced angiogenesis. *Biochimica et Biophysica Acta (BBA): General Subjects*, *1722*(1), 22–29.

Hu, F. Q., Liu, L. N., Du, Y. Z. & Yuan, H. (2009). Synthesis and antitumor activity of doxorubicin conjugated stearic acid-G-chitosan oligosaccharide polymeric micelles. *Biomaterials*, *30*(36), 6955–6963.

Hu, F. Q., Ren, G. F., Yuan, H., Du, Y. Z. & Zeng, S. (2006). Shell cross-linked stearic acid grafted chitosan oligosaccharide self-aggregated micelles for controlled release of paclitaxel. *Colloids and Surfaces B: Biointerfaces*, *50*(2), 97–103.

Hu, F. Q., Zhao, M. D., Yuan, H., You, J., Du, Y. Z. & Zeng, S. (2006). A novel chitosan oligosaccharides–stearic acid micelles for gene delivery: Properties and in vitro transfection studies. *International Journal of Pharmaceutics*, *315*(1–2), 158–166.

Kim, D., Choi, C., Jeong, Y., Jang, M. & Nah, J. (2006). All-trans retinoic acid-associated low molecular weight water-soluble chitosan nanoparticles based on ion complex. *Macromolecular Research*, *14*(1), 66–72.

Kucukzeybek, Y., Gul, M. K., Cengiz, E., Erten, C., Karaka, B., Gorumlu, G., et al. (2008). Enhancement of docetaxel-induced cytotoxicity and apoptosis by all-trans retinoic acid (ATRA) through downregulation of survivin (Birc 5), Mcl-1 and Ltbeta-R in hormone- and drug resistant prostate cancer cell line, Du-145. *Journal of Experimental and Clinical Cancer Research*, *27*(1), 1–8.

Lee, K. Y., Kwon, I. C., Kim, Y. H., Jo, W. H. & Jeong, S. Y. (1998). Preparation of chitosan self-aggregates as a gene delivery system. *Journal of Controlled Release*, *51*(2–3), 213–220.

Lee, H., Lee, K. & Park, T. G. (2008). Hyaluronic acid–paclitaxel conjugate micelles: Synthesis, characterization, and antitumor activity. *Bioconjugate Chemistry*, *19*(6), 1319–1325.

Li, Y., Qi, X. R., Maitani, Y. & Nagai, T. (2009). Peg–Pla diblock copolymer micelle-like nanoparticles as all-trans-retinoic acid carrier: In vitro and in vivo characterizations. *Nanotechnology*, *20*(5), 1–10.

Li, Y., Zhang, S., Meng, X., Chen, X. & Ren, G. (2010). The preparation and characterization of a novel amphiphilic oleoyl-carboxymethyl chitosan self-assembled nanoparticles. *Carbohydrate Polymers*, *83*(1), 130–136.

Lin, L. M., Li, B. X., Xiao, J. B., Lin, D. H. & Yang, B. F. (2005). Synergistic effect of all-trans-retinoic acid and arsenic trioxide on growth inhibition and apoptosis in human hepatoma, breast cancer, and lung cancer cells in vitro. *World Journal of GastroEnterology*, *11*(36), 5633–5637.

Liu, C. G., Chen, X. G. & Park, H. J. (2005). Self-assembled nanoparticles based on linoleic-acid modified chitosan: Stability and adsorption of trypsin. *Carbohydrate Polymers*, *62*(3), 293–298.

Liu, J., Li, H., Jiang, X., Zhang, C. & Ping, Q. (2010). Novel pH-sensitive chitosan derived micelles loaded with paclitaxel. *Carbohydrate Polymers*, *82*(2), 432–439.

López-León, T., Carvalho, E. L., Seijo, B., Ortega-Vinuesa, J. L. & Bastos-González, D. (2005). Physicochemical characterization of chitosan nanoparticles: Electrokinetic and stability behavior. *Journal of Colloid and Interface Science*, *283*(2), 344–351.

Loretz, B. & Bernkop-Schnürch, A. (2006). In vitro evaluation of chitosan–EDTA conjugate polyplexes as a nanoparticulate gene delivery system. *The AAPS Journal*, *8*(4), 756–764.

Lübbert, M., Müller Tidow, C., Hofmann, W. K. & Koeffler, H. P. (2008). Advances in the treatment of acute myeloid leukemia: From chromosomal aberrations to biologically targeted therapy. *Journal of Cellular Biochemistry*, *104*(6), 2059–2070.

Lv, H., Zhang, S., Wang, B., Cui, S. & Yan, J. (2006). Toxicity of cationic lipids and cationic polymers in gene delivery. *Journal of Controlled Release*, *114*(1), 100–109.

Mao, W. G., Liu, Z. L., Chen, R., Li, A. P. & Zhou, J. W. (2006). Jwa is required for the antiproliferative and pro apoptotic effects of all trans retinoic acid in hela cells. *Clinical and Experimental Pharmacology and Physiology*, *33*(9), 816–824.

Muzzarelli, R. A. A., Orlandini, F., Boselli, E., Frega, N. G., Tosi, G. & Muzzarelli, C. (2006). Chitosan taurocholate capacity to bind lipids and to undergo enzymatic hydrolysis: An in vitro model. *Carbohydrate Polymers*, *66*(3), 363–371.

Na, K., Park, K. H., Kim, S. W. & Bae, Y. H. (2000). Self-assembled hydrogel nanoparticles from curdlan derivatives: Characterization, anti-cancer drug release and interaction with a hepatoma cell line (Hepg2). *Journal of Controlled Release*, *69*(2), 225–236.

Nishiyama, N., Bae, Y., Miyata, K., Fukushima, S. & Kataoka, K. (2005). Smart polymeric micelles for gene and drug delivery. *Drug Discovery Today: Technologies*, *2*(1), 21–26.

Schug, T. T., Berry, D. C., Shaw, N. S., Travis, S. N. & Noy, N. (2007). Opposing effects of retinoic acid on cell growth result from alternate activation of two different nuclear receptors. *Cell*, *129*(4), 723–733.

Seo, S. J., Kim, S. H., Sasagawa, T., Choi, Y. J., Akaike, T. & Cho, C. S. (2004). Delivery of all trans-retinoic acid (RA) to hepatocyte cell line from RA/galactosyl [alpha]-cyclodextrin inclusion complex. *European Journal of Pharmaceutics and Biopharmaceutics*, *58*(3), 681–687.

Tang, X. H. & Gudas, L. J. (2011). Retinoids, retinoic acid receptors, and cancer. *Annual Review of Pathology*, *6*, 345–364.

Veronese, F. M., Schiavon, O., Pasut, G., Mendichi, R., Andersson, L., Tsirk, A., et al. (2005). PEG–doxorubicin conjugates: Influence of polymer structure on drug release, in vitro cytotoxicity, biodistribution, and antitumor activity. *Bioconjugate Chemistry*, *16*(4), 775–784.

Wolszczak, M. & Miller, J. (2002). Characterization of non-ionic surfactant aggregates by fluorometric techniques. *Journal of Photochemistry and Photobiology A: Chemistry*, *147*(1), 45–54.

Ye, Y. Q., Hu, F. Q. & Yuan, H. (2004). Preparation and characterization of stearic acid-grafted chitosan oligosaccharide polymeric micelles. *Yao Xue Xue Bao*, *39*(6), 467–471.

Yokoyama, M., Okano, T., Sakurai, Y., Suwa, S. & Kataoka, K. (1996). Introduction of cisplatin into polymeric micelle. *Journal of Controlled Release*, *39*(2–3), 351–356.

Yoo, H. S. & Park, T. W. (2001). Biodegradable polymeric micelles composed of doxorubicin conjugated PLGA–PEG block copolymer. *Journal of Controlled Release*, *70*(1–2), 63–70.

Yuan, X. B., Li, H. & Yuan, Y. B. (2006). Preparation of cholesterol-modified chitosan self-aggregated nanoparticles for delivery of drugs to ocular surface. *Carbohydrate Polymers*, *65*(3), 337–345.

Zhang, C., Ping, Q., Zhang, H. & Shen, J. (2003). Preparation of N-alkyl-O-sulfate chitosan derivatives and micellar solubilization of taxol. *Carbohydrate Polymers*, *54*(2), 137–141.